OXFORD

ORIGINAL ARTICLE

Diminished Myoinositol in Ventromedial Prefrontal Cortex Modulates the Endophenotype of Impulsivity

Bianca Jupp[1], Steve J. Sawiak[2], Bastiaan van der Veen[1], Suzanne Lemstra[1], Chiara Toschi[1], Rebecca L. Barlow[3], Anton Pekcec[3], Tom Bretschneider[3], Janet R. Nicholson[3], Trevor W. Robbins[1], and Jeffrey W. Dalley[1,4,*]

[1]Department of Psychology, University of Cambridge, Cambridge CB2 3EB, UK, [2]Department of Physiology, Development and Neuroscience, University of Cambridge, Cambridge, UK, [3]Boehringer Ingelheim Pharma GmbH & Co. KG, Biberach an der Riss 88397, Germany, and [4]Department of Psychiatry, Addenbrooke's Hospital, University of Cambridge, Cambridge CB2 2QQ, UK

Address correspondence to Professor Jeffrey W. Dalley, Department of Psychology, University of Cambridge, Downing St, Cambridge CB2 3EB, UK.
Email: jwd20@cam.ac.uk.

Abstract

Maladaptive impulsivity manifests in a variety of disorders, including attention-deficit hyperactivity disorder (ADHD), depression, and substance use disorder. However, the etiological mechanisms of impulsivity remain poorly understood. In the present study, we used in-vivo proton magnetic resonance spectroscopy (^{1}H-MRS) to investigate neurometabolite content in the prefrontal cortex (PFC) and striatum of rats exhibiting low- versus high-impulsive (LI, HI) behavior on a visual attentional task. We validated our ^{1}H-MRS findings using regionally resolved ex-vivo mass spectroscopy, transcriptomics, and site-directed RNA interference in the ventromedial PFC. We report a significant reduction in myoinositol levels in the PFC but not the striatum of HI rats compared with LI rats. Reduced myoinositol content was localized to the infralimbic (IL) cortex, where significant reductions in transcript levels of key proteins involved in the synthesis and recycling of myoinositol (IMPase1) were also present. Knockdown of IMPase1 in the IL cortex increased impulsivity in nonimpulsive rats when the demand on inhibitory response control was increased. We conclude that diminished myoinositol levels in ventromedial PFC causally mediate a specific form of impulsivity linked to vulnerability for stimulant addiction in rodents. Myoinositol and related signaling substrates may thus offer novel opportunities for treating neuropsychiatric disorders comorbid with impulsive symptomology.

Key words: attention-deficit hyperactivity disorder, inositol monophosphatase 1 (IMPA1), inositol-triphosphate (IP$_3$), magnetic resonance spectroscopy, prefrontal cortex

Introduction

Impulsivity refers to the propensity for rapid, unduly risky, poorly planned, and prematurely expressed behavior (Evenden 1999; Moeller et al. 2001; Dalley and Robbins 2017). As a widely studied endophenotype associated with substance use disorder (Jentsch and Taylor 1999; Ersche et al. 2010),

and as a core manifestation of attention-deficit hyperactivity disorder (ADHD), impulsivity is recognized as a multivariate neurobehavioral construct in humans and experimental animals (Winstanley et al. 2006; Voon and Dalley 2016). Based on much empirical support, several distinct subtypes of impulsivity have been identified, including the dichotomies of "waiting"

and "stopping" impulsivity (Robinson et al. 2009), "action" and "choice" impulsivity (Winstanley et al. 2006), "restraint" and "cancelation" impulsivity (Schachar et al. 2007), which each engage separable but partially overlapping neural networks (Dalley et al. 2011) and pharmacological mechanisms (Pattij and Vanderschuren 2008). In particular, the construct of waiting impulsivity—the inability to withhold responding for a signaled reward following an unpredictable or unexpected delay—is an endophenotype strongly linked with substance use disorder (Dalley and Ersche 2019).

The capacity to restrain responding can be assessed in rodents using computerized behavioral paradigms, including the stop-signal reaction time task, go/no-go tasks, and other motor inhibition tasks based on differential rates of low reinforcement schedules and the 5-choice serial reaction time task (5CSRTT) (Evenden 1999). Such tasks depend on dopamine, norepinephrine, and serotonin (5-HT) operating at distinct cortical and subcortical loci (Dalley and Roiser 2012). For example, excessive premature responding on the 5CSRTT or the equivalent 1-hole reaction time task—an operational measure of one form of waiting impulsivity—is associated with low D2 receptor availability in the ventral striatum and increased 5-HT release in the prefrontal cortex (PFC) (Dalley et al. 2002, 2007; Jupp et al. 2013). However, increasingly, the etiology of impulsivity is recognized to involve neural circuits and mechanisms beyond the monoamine systems. For example, impulsivity on the 5CSRTT is predicted by γ-amino-butyric acid (GABA) and morphological deficits in the NAcb (Caprioli et al. 2014) and insular cortex (Belin-Rauscent et al. 2016) suggesting that local circuit-level perturbations in cortical and subcortical regions may play a role in the genesis of this behavior.

Magnetic resonance spectroscopy (MRS) is a noninvasive, clinically relevant and translatable neuroimaging methodology used widely to assess the relative concentration of key neurochemicals underlying metabolic processes and neuro-transmitter composition within experimentally selected regions of the brain (Boy et al. 2011; Godlewska et al. 2017). To date, however, few studies have used this approach to investigate neurochemical and metabolic biomarkers associated with impulsivity in clinical populations (reviewed in (Naaijen et al. 2015)) or impulsivity traits in experimental animals. Thus, in the present study, we used in-vivo proton (^{1}H) MRS to quantify neurometabolite content in the PFC and striatum of rats phenotyped for trait high or low levels of impulsive responding on the 5CSRTT. Trait-like impulsivity on this task predicts several features of substance use disorder, including an increased propensity for escalation, relapse, and compulsive drug seeking and taking (Dalley et al. 2007; Belin et al. 2008; Diergaarde et al. 2008; Economidou et al. 2009). We validated our neurochemical findings with direct neurometabolite measurement by mass spectrometry (MS), local gene transcription, and selective silencing of genes associated with the synthesis and turnover of identified candidate neurometabolites.

Materials and Methods

Experimental Subjects

Subjects were 288 male, Lister-hooded rats, weighing 280–300 g at the start of the experiment. Water was available ad libitum and sufficient food was provided to maintain body weights at no less than 90% of free-feeding weights for the duration of the study (18–20 g chow/day). Rats were housed under temperature- and humidity-controlled conditions and a reversed 12-h light/dark cycle (white lights off/red light on at 07:00 h). Rats destined for ex-vivo mass spectroscopy analysis ($n = 48$) were housed under identical conditions with experimental procedures authorized by the Local Animal Care and Use Committee at Boehringer Ingelheim Inc. and the USDA Animal Welfare Act. Experiments in the UK were in accordance with the UK (1986) Animal (Scientific Procedures) Act and were approved by the University of Cambridge Animal Welfare and Ethical Review Body (AWERB).

Behavioral Training and Impulsivity Screening

Rats were trained daily on the 5CSRTT using apparatus (Med Associates Inc) controlled by WhiskerServer and FiveChoice client software (Cardinal and Aitken 2010), as described previously (Bari et al. 2008). Training sessions consisted of 100 discrete trials or 30 min, whichever elapsed first. Each trial was initiated by the entry of the animal into the food magazine. Following an intertrial interval (ITI) of 5 s, a brief light stimulus (0.7 s in duration) was presented on a random basis in one of the five apertures. A nose poke into the corresponding aperture was rewarded with delivery of one food pellet (TestDiet). Failure of the animal to respond within 5 s (omission), a nose poke into the incorrect aperture (incorrect response) or prior to the presentation of the light stimulus (premature response) resulted in a 5 s time-out, during which time the house light was extinguished, and no new trials could be initiated. Daily training sessions, 6 days a week, continued until acquisition of stable responding (response accuracy $\leq 75\%$, omissions $\leq 20\%$) at which point animals were challenged with a series of long ITI sessions, during which time the ITI was increased to 7 s to increase the number of premature responses across these sessions. A challenge session was employed once every five sessions, on three occasions. Rats were ranked for their level of impulsivity based on the number of premature responses across the three challenge sessions, as described previously (Dalley et al. 2007). Rats expressing on average $\geq 50\%$ premature responses were deemed high impulsive while those expressing $\leq 30\%$ premature responses were considered low impulsive. An equal number of HI and LI rats were included in each phase of the experiment. Rats across all three cohorts demonstrated significant differences in the number of premature responses ($F(2,46) = 9.7$, $P = 0.0003$) and discriminative attentional accuracy ($F(2,46) = 6.2$, $P = 0.004$) with no significant difference in the number of omissions ($F(2,46) = 1.2$, $P = 0.3$) (Table 1). Given these cohort-specific effects, we were therefore unable to determine the relationship between the various in-vivo- and ex-vivo-dependent variables of this study. We thus restricted our analyses of HI versus LI contrasts to each individual cohort.

^{1}H Magnetic Resonance Spectroscopy

Proton magnetic resonance spectroscopy (^{1}H-MRS) was conducted using a 4.7 T small-animal spectrometer run with Paravision 5.1 software (Bruker Biospec). Twelve HI and 12 LI rats were scanned under isoflurane-induced general anesthesia (1.5–2.5% in 1 l/min medical O$_2$) with continuous physiological monitoring (breathing rate, heart rate, body temperature, and oxygen saturation) throughout the duration of the experiment. Anesthetic dose rates were adjusted to keep respiration rates within an appropriate physiological range (50–70 cycles/min), and body temperature was maintained at 37°C with a water heating pad.

Table 1 A summary of the behavioral variables assessed during the three long ITI sessions used to screen for the HI and LI phenotypes

	Premature responses[*],[**],[***]		Correct responses[*],[**]		Omissions[***]	
	HI	LI	HI	LI	HI	LI
^{1}H-MRS $n = 96$ 12HI/12LI	65.39 ± 3.43	26.44 ± 1.01	76.99 ± 1.37	79.61 ± 1.51	8.64 ± 1.51	8.56 ± 1.16
MS $n = 48$ 6HI/6LI	60.88 ± 4.76	17.72 ± 1.08[a]	71.00 ± 1.26	78.82 ± 2.82	4.88 ± 0.90[a]	12.60 ± 2.01
qRTPCR $n = 96$ 8HI/8LI	63.14 ± 4.55	18.96 ± 1.49[a]	78.73 ± 5.56[b]	84.45 ± 1.98	12.60 ± 2.07[b]	7.71 ± 1.07

In total, three cohorts of rats were trained and screened for impulsivity; these were subsequently used for magnetic resonance spectroscopy (^{1}H-MRS), MS and quantitative real time PCR (qRTPCR).
[*]$P < 0.05$ main effect of impulsivity.
[**]$P < 0.05$ main effect of cohort.
[***]$P < 0.05$ interaction, two-way ANOVA.
[a]$P < 0.05$ vs. MRS.
[b]$P < 0.05$ vs. MS, Sidak post hoc comparison.

Scans were acquired using a 72 mm birdcage transmit coil (Bruker model T2000V3) and a 4-channel array for reception (Bruker model T13014). Localizer and rapid acquisition with relaxation enhancement images were first acquired (repetition time 15.3 s, effective echo time 36 ms, echo train length 8, field of view 64×64 mm^2, matrix 256×256 for 250 µm planar resolution with 250 µm slice thickness in 6 min 7 s) to guide placement of the voxel of interest for MRS measurement. A PRESS (point resolved spectroscopy) protocol was acquired in two locations: PFC and striatum (Fig. 1). Automated adjustments were conducted for receive frequency and transmit power. An automated image-based shimming routine (MAPSHIM) and manual adjustment of water suppression pulses (VAPOR) were performed for each voxel prior to acquisition. Metabolite concentrations were calculated using LCModel (Provencher 2001) and normalized to creatinine-containing metabolites (creatinine + phosphocreatine; Cr + PCr). Assessed metabolites were considered reliable and included in analysis where the estimated Cramér-Rao lower bound (CRLB) value calculated by LCModel was within 20%.

Ex-vivo Analysis of Myoinositol

To validate the findings of the ^{1}H-MRS study, tissue microdissections of PFC subregions (infralimbic cortex, prelimbic cortex, and anterior cingulate cortex) were analyzed using MS to assess myoinositol levels in a separate cohort of HI ($n = 6$) and LI ($n = 6$) rats. Following screening for impulsivity, animals were terminally anesthetized with sodium pentobarbital (1.5 mL, 200 mg/mL i.p.) and decapitated. Brains were then rapidly excised and frozen over liquid nitrogen. All brains were stored at $-80°C$ until use. Bilateral tissue microdissections (1 mm × 150 µm) of target regions-of-interest were collected from coronal cryo-sections cut on a CM300 cryostat (Leica) and weighed before being stored at $-80°C$ until further processing.

Solvents were purchased from Fisher Scientific and plastic consumables from Eppendorf. Chemical reference compounds were purchased from Sigma-Aldrich. Brain punches were homogenized in water with a Precellys tissue homogenizer (Bertin) in a 1:50 ratio. Ten µL of the homogenate was spiked with 20 µL of 400 µM myo-inositol-C-d$_6$ (internal standard). Protein was precipitated by addition of 100 µL acetonitrile/methanol (50:50), freezing for 10 min at $-20°C$ and subsequent centrifugation at 4000 rpm, 4°C for 10 min. Twenty µL of the supernatant was injected into the liquid chromatography—MS system. Calibrants in the range of 0.2–200 µM were prepared in water. A triple quadrupole 6500 (AB Sciex) MS was equipped with an autosampler and liquid-chromatography (LC) 1200 (Agilent) system. The instrument operated in negative mode and the following transitions were recorded: myo-inositol Q1 = 179.0, Q3 = 87.0, DP = −80, CE = −5; N-acetylaspartic acid (NAA), Q1 = 173.9, Q3 = 88.1, DP = −15, CE = −22 and myo-inositol-C-d6 Q1 = 185.0, Q3 = 92, DP = −80, CE = −12. Analytes were separated on a Luna NH2 5 µm, 150×2 mm column (Phenomenex). Solvent A was composed of 20 mM ammonium acetate, 20 mM ammonium hydroxide in 95:5 water/acetonitrile (pH 9); solvent B was 100% acetonitrile. The LC gradient started at 85% solvent B, maintained for 0.7 min, and then decreased to 2% for 1 min. For reequilibration, solvent B was set to 85% for 1.5 min. Myoinositol concentration was normalized to NAA concentration to account for differences in tissue content between samples and averaged across duplicate samples. Duplicate samples which showed greater than 20% standard deviation in concentration were excluded from further analysis.

Quantitative Real Time PCR

To investigate whether the observed reduction in myoinositol was associated with deficits in synthesis and/or transport, transcript levels were assayed for proteins involved in myoinsoitol production (inositol-3-phosphate synthase 1, ISYNA1; inositol monophosphatase 1, IMPase1), uptake (sodium myoinositol intracellular transporter 1, SMIT1), and breakdown (CDP-diacylglycerol-inositol 3-phosphatidyltransferase, CDIPT), within the infralimbic cortex of a separate cohort of rats screened on the 5CSRTT (Cohort 3: HI, $n = 8$; LI $n = 8$). Since myoinositol has been implicated as a putative glial marker (Griffin et al. 2002), and given that glucose is a precursor for myo-inositol synthesis, we additionally assessed the levels of glial fibriliary acidic protein (GFAP) and the two brain glucose transporters (GLUT1 and GLUT3).

Following screening for impulsivity phenotypes, rats were terminally anesthetized with sodium pentobarbital (1.5 mL, 200 mg/mL i.p.). Following decapitation, brains were rapidly excised, frozen over liquid nitrogen, and stored at $-80°C$ until use. Tissue microdissections (1 mm × 300 µm) targeting the infralimbic and prelimbic cortex were collected from coronal cryo-sections cut on a CM300 cryostat (Leica) and stored at $-80°C$ until further use. Messenger RNA was extracted from the frozen samples using the RNeasy Micro Kit (Qiagen) and reverse transcribed using the RT2 first strand kit (Qiagen) according to the manufacturer's protocol. qRT-PCR amplification was performed using a QFX96 PCR detection system (Biorad) with the use of RT2 SYBER Green Master Mix (Qiagen) with RT2 qPCR primer assay for each gene of interest (Qiagen). *ACTB*, *HPRT*, and
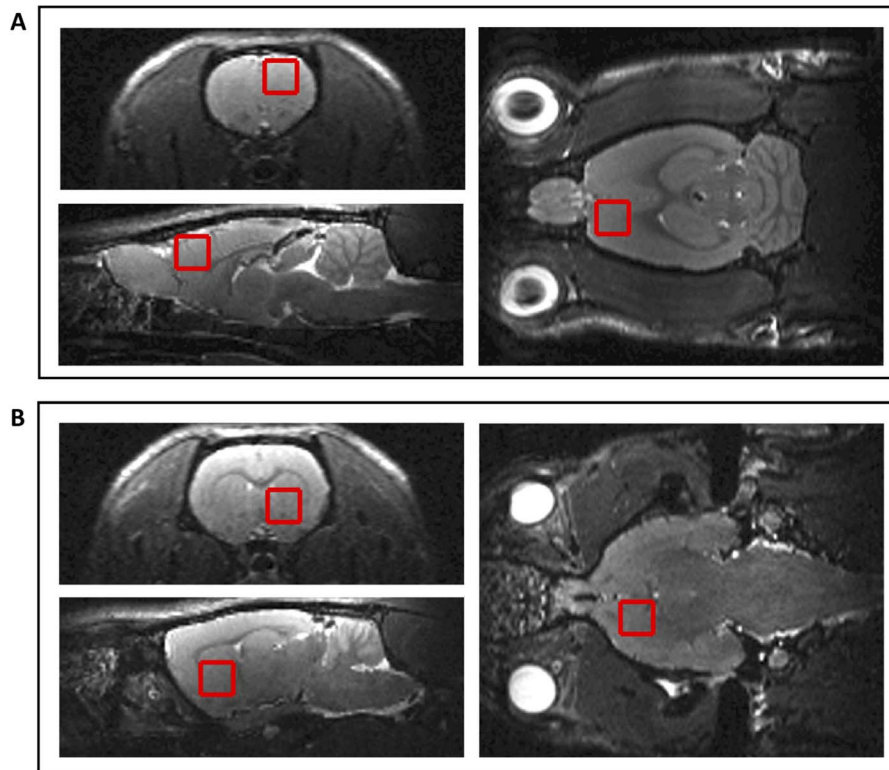
Figure 1. Representative voxel positions for ^{1}H-MRS. (A) PFC (B) striatum.

TBP were used as housekeeping genes and samples were run in duplicate. On occasions where duplicate samples showed greater than 20% standard deviation in expression these were excluded from further analysis. Relative gene expression was calculated using the delta Ct method.

siRNA-Mediated Knockdown of IMPase1

Under isoflurane anesthesia (1.5–2% in medical air), nine non-impulsive rats (mean premature responses during three long-ITI sessions <50) from a separate cohort of rats (Cohort 4) were implanted with bilateral 22-gage double-lumen guide cannulae (Plastics One) above the infralimbic cortex. Stereotaxic coordinates relative to bregma were: anterior-posterior +3.0 mm, medial-lateral ±0.75 mm, and dorsal-ventral −2.2 mm (Paxinos and Watson 2007). Guide cannula were occluded by a stylet and secured to the skull with dental cement and stainless-steel screws.

Following a 1-week recovery period, animals were retrained on the 5CSRTT and rechallenged across a series of LITI sessions to ensure baseline premature responding was consistent across the cohort, affected as a result of implantation of the cannula (Chudasama et al. 2003). Rats then received bilateral infusions of siRNA targeting IMPase1 (*n* = 5, ON-TARGETplus SMARTpool, Dharmacon Inc.), or a nontargeting control siRNA (*n* = 4, Dharmacon Inc.), diluted in polyethyleneimine (in-vivo jet-PEI, Polyplus Transfection). Each 1 μL microinfusion contained 0.5 μg/μL siRNA and was delivered at 0.1 μL/min into the infralimbic cortex under isoflurane anesthesia (1.5% in medical air) on two consecutive days. Training sessions were again resumed the day following the final siRNA infusion and continued 6 days a week throughout the experimental period.

Behavioral Consequences of IMPase1knockdown

Three days after the final siRNA infusion, performance on the 5CSRTT was evaluated using a variable ITI session consisting of 40 trials each of 5, 7, and 9 s ITIs. This session, incorporating unpredictable waiting intervals, selectively challenged inhibitory control processes when transcript knockdown was considered maximal (Karatas et al. 2013). Following a washout period of 3 weeks, after which time recovery of expression was assumed to be complete (Batassa et al. 2010), siRNA treatment was reversed such that rats that had previously received targeted siRNA were infused with control siRNA and vice versa. Behavioral performance on the 5CSRTT was again assessed 3 days after the final siRNA infusion. For one animal infused with targeted siRNA, a technical fault in the behavioral apparatus precluded the inclusion of their data in the final analysis.

At the end of the behavioral assessment, rats were terminally anesthetized with sodium pentobarbitone (1.5 mL, 200 mg/mL, i.p.) and perfused transcardially with 100 mL 0.1 M PBS followed by 400 mL 4% paraformaldehyde (Sigma). Brains were postfixed overnight in 4% paraformaldehyde, and cryoprotected in 20% sucrose in PBS for 24 h, prior to being frozen over liquid nitrogen and stored at −80°C. Serial 50 μm cryo-sections sampling the entire PFC were then collected and examined to reconstruct the location of cannula in the PFC. Two of the nine animals were excluded from the study due to incorrect cannula placement.

Validation of IMPase1knockdown

To validate the efficacy of siRNA-mediated inhibition of IMPase1 transcript expression, a behaviorally naive cohort of rats (*n* = 12) was implanted with bilaterally indwelling cannula overlying the infralimbic cortex. Following 1 week of recovery, rats received

either siRNA targeting IMPase1 ($n = 6$) or nontargeting siRNA ($n = 6$), as described above. Five days following the final siRNA infusion, corresponding to the same time point that the variable intertrial interval (vITI) was assessed, rats were terminally anesthetized with sodium pentobarbital (1.5 mL, 200 mg/mL i.p.), decapitated, and their brains rapidly excised and frozen over liquid nitrogen. Brains were stored at −80°C until further processing. Tissue microdissections (1 mm × 300 μm) targeting the infralimbic cortex were collected from 300 μm cryo-sections. RNA was prepared and IMPase1 expression assessed using qRT-PCR, as described above.

Statistical Analysis

Statistical analyses were carried out using SPSS (IBM version 23). Rats were classified as LI versus HI according to the numerical classification described above. Task variables (premature responses, accuracy, and omissions) were averaged across the three long LITI sessions and compared between HI and LI rats by two-way ANOVA with impulsivity phenotype as the between subject's factor (HI and LI) and cohort as the within subject's variable. Homogeneity of variance was verified using Levene's test whilst normality was assessed by the Shapiro Wilk's test. Where homogeneity of variance was violated, statistical analyses were conducted on log transformed data. Differences in in-vivo and post mortem levels of neurometabolites were assessed by independent Student's t-tests. Consistent with previous exploratory ^{1}H-MRS studies of rodent behavior (e.g., Yoo et al. 2018), t-tests were conducted without correction for multiple comparisons, and while the application of this statistical analysis should be interpreted with caution given the increased likelihood of type I error, this approach accounts for the relatively low subject numbers available for the study. Gene transcripts were clustered together as either those involved in myoinositol transport, synthesis, and recycling through the IP3 pathway (CDIPT, SMIT1, and IMPA1) or involved in the de novo synthesis of myo-inositol from its precursor glucose, which also included glucose handling and glial markers (ISYNA1, GLUT1, 3 and GFAP). Transcript data were analyzed by two-way ANOVA with impulsivity phenotype as the between subject's factor (HI and LI) and transcript as the within subject's variable. The effect of transcript knockdown on performance on the 5CSRTT was assessed using a repeated measures mixed effects model ANOVA with treatment as the between subject's factor (control, knockdown) and ITI (5s, 7s, 9s) as the within subject's factor. Post hoc analyses were performed using Sidak's procedure. Statistical significance was set at $P < 0.05$.

Results

Trait Impulsive Rats Show a Reduction in Myoinositol Content in the PFC

We first used ^{1}H-MRS to profile key neurometabolites in the PFC and ventral striatum of rats stratified for extreme low versus high impulsivity in the 5CSRTT. Using this imaging approach, we assessed neuronal integrity (NAA), glial cellular (myoinositol) and microtubule markers (taurine, Tau), glutamate metabolism (glutamate, Glu; glutamine, Gln), antioxidants (glutathione, GSH), and choline metabolites (glycerophosphorylcholine, GPC; phosphocholine, PCh) as well as glucose (Glc). This analysis revealed that myoinositol content in the PFC volume of interest was significantly reduced in HI rats compared with LI rats

Table 2 Relative concentration of neurometabolites in the PFC as detected by ^{1}H-MRS

Metabolite	LI $n = 12$	HI $n = 12$
NAA	0.90 ± 0.04	0.89 ± 0.02
Ins	0.72 ± 0.02	0.63 ± 0.03*
Glu	1.62 ± 0.03	1.60 ± 0.03
Gln	0.73 ± 0.03	0.72 ± 0.04
GSH	0.43 ± 0.02	0.43 ± 0.02
Tau	0.73 ± 0.04	0.75 ± 0.03

Myoinositol (Ins) concentration was significantly lower in the PFC of HI rats. No significant differences were observed for any other metabolites.
* $P < 0.05$.

Table 3 Relative concentration of neurometabolites in the striatum as detected by ^{1}H-MRS

Metabolite	LI $n = 12$	HI $n = 12$
NAA	0.75 ± 0.02	0.81 ± 0.02
Ins	0.79 ± 0.03	0.81 ± 0.02
Glu	1.35 ± 0.03	1.39 ± 0.03
Gln	0.75 ± 0.03	0.73 ± 0.04
GSH	0.37 ± 0.02	0.37 ± 0.02
Tau	0.88 ± 0.04	0.92 ± 0.03

No significant differences were observed for any metabolites in this region.

($t = 2.183$, $P = 0.04$, Fig. 2A). However, when applying a statistical test to account for multiple comparisons (two-way ANOVA with Sidak's multiple comparison test), this effect was no longer significant ($P = 0.17$). The trend reduction in in-vivo myoinositol concentration was neurochemically and regionally selective with no significant differences in other neurometabolites in this region or within the striatum (Tables 2 and 3). Given that the PFC voxel encompassed functionally distinct regions of the PFC known differentially to contribute to impulsivity, we next used ex-vivo MS in a separate cohort of rats to measure myoinositol levels directly in the prelimbic (PrL), infralimbic (IL), and anterior cingulate cortices (ACC) of HI and LI rats. We found that myoinositol content was significantly reduced in the IL cortex of HI animals compared with LI rats ($t = 4.286$, $P < 0.01$; Fig. 2D) but was no different between HI and LI rats in the ACC and PrL (Fig. 2B,C). Thus, using two complementary approaches, our findings show that myoinositol content is significantly and selectively diminished in the IL cortex of HI rats.

Transcript Levels of Proteins Involved in Myoinositol Synthesis and Transport are Reduced in the Infralimbic Cortex of HI Rats

To determine the origin of the observed reduction in myoinositol content in the IL cortex of HI rats, we next measured local transcript levels of proteins involved in the transport (SMIT1), synthesis (IMPase1), and recycling (CDIPT) of myoinositol through the IP3 pathway, as well as transcripts of transporters for glucose (glucose transporter 1, GLUT1, GLUT3), and glial cellular function (glial fibrillary acidic protein, GFAP) in this region. A main effect of impulsivity was observed for transcripts involved in the transport, synthesis, and recycling of myoinositol through the IP3 pathway ($F(1,37) = 21.31$, $P < 0.0001$), with post hoc analysis revealing a significant reduction in the expression of IMPase1 in
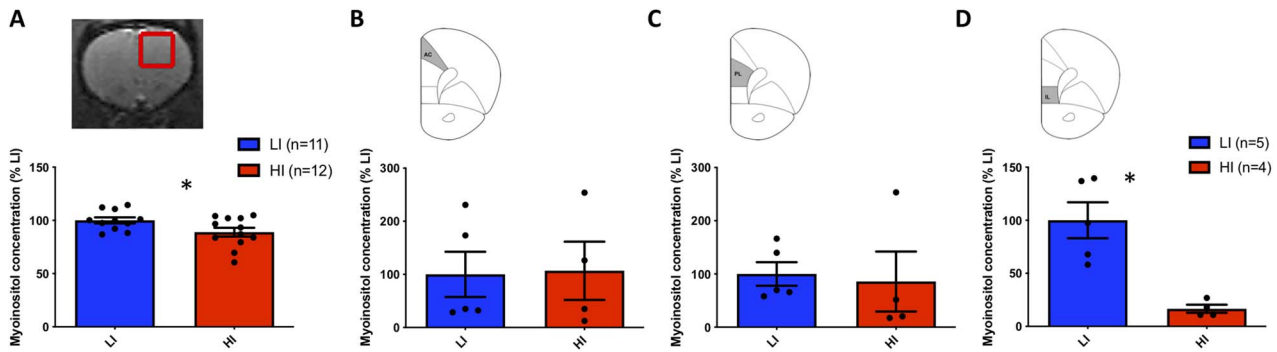
Figure 2. Relative myoinositol concentration within the PFC from ^{1}H-MRS and mass spectroscopy studies in high (HI) and low (LI) impulsive rats. (A) In-vivo myoinositol concentration was significantly reduced as detected by magnetic resonance spectroscopy in the PFC of HI rats. Direct measurement of myoinositol in microdissected subregions of the PFC using mass spectroscopy revealed no significant changes in myoinositol content within the anterior cingulate (AC) (B) and prelimbic (PrL) (C) cortices. By contrast, myoinositol levels were significantly reduced within the infralimbic cortex (IL) of HI versus LI rats (D). Data are expressed as a percentage of normalized myoinositol concentration in LI rats,* denotes $P < 0.05$.

the IL cortex of HI rats ($t = 3.633$, $P < 0.01$) (Fig. 3B). No significant differences in gene expression were identified for transcripts involved in de novo synthesis of myoinositol from its precursor glucose, glucose handling, or the glial marker GFAP within this region (Fig. 3C). We also observed no significant differences in transcript expression of IMPase1, CDIPT, and SMIT1 in the PrL cortex of HI and LI rats (Fig. 3D).

Knockdown of IMPase1 Expression in the Infralimbic Cortex Increases Impulsive Responding

To investigate whether a diminished capacity for myoinositol synthesis within the IL cortex causally modulates impulsivity, we inhibited transcript expression of IMPase1 using a siRNA approach. Knockdown of this transcript significantly increased premature responding on a vITI challenge specifically at the 9s ITI (ITI: $F(2,12) = 168.7$, $P < 0.0001$; treatment: $F(1,6) = 24.91$, $P = 0.025$; ITI × treatment interaction: $F(2,9) = 60.93$, $P = 0.0001$, post hoc test 9 s ITI $t = 11.1$, $P < 0.0001$; Fig. 4D). This consequence of IMPase knockdown was behaviorally selective with no significant effects on other task variables, including attentional accuracy, response latencies, and omissions (Fig. 4E–G). To confirm the observed effect of IMPase knockdown was not influenced by the cross-over experimental design, secondary statistical analysis comparing premature responding at 9s between animals receiving either knockdown or control siRNA as the first or second treatment revealed a main effect of treatment $F(3,9) = 5.580$, $P = 0.019$, ANOVA). Post hoc analyses found no significant differences in premature responding in animals within each control (control 1 vs. control 2, $q = 1.252$, $P > 0.8$) and knockdown groups (knockdown 1 vs. knockdown 2, $q = 2.898$, $P > 0.2$), with significant or near significant differences between all control and knockdown groups (control 1 vs. knockdown 1, $q = 4.01$, $P = 0.06$; control 1 vs. knockdown 2, $q = 4.19$, $P = 0.06$; control 2 vs. knockdown 1, $q = 3.721$, $P = 0.09$, control 2 vs. knockdown 2, $q = 5.521$, $P = 0.01$). These analyses confirm that there was no effect of treatment order on the reported behavioral effects.

We next validated the siRNA approach by evaluating IMPase1 expression after targeted siRNA administration in the IL cortex at the same corresponding time point as the vITI challenge in a separate cohort of naive rats. We confirmed that locally administered siRNA resulted in a significant reduction in IMPase1expression in the IL cortex ($t = 2.913$, $P = 0.009$), corresponding to an approximate 50% decrease compared to

transcript expression following treatment with the nontargeting control siRNA (Fig. 4C).

Discussion

The main findings of this study demonstrate that impulsive responding on the 5CSRTT in rats is associated with reduced levels of myoinositol in the IL cortex, an area equivalent phylogenetically to Brodmann area 25 in humans (Uylings et al. 2003; Vertes 2004; Gabbott et al. 2005). Our findings indicate that diminished myoinositol levels may have been caused by a reduction in the capacity for the synthesis and/or recycling of this key signaling compound in the IL cortex, as indicated by a reduction in transcript expression of the main enzyme involved in these processes, IMPase1. Thus, knocking down the expression of IMPase1 within the IL cortex was sufficient to increase impulsive responding under conditions of uncertainty in otherwise nonimpulsive rats. These findings collectively reveal a relationship between reduced myoinositol signaling in the ventromedial PFC and increased impulsivity. Reduced myoinositol content and function in homologous areas of human PFC may therefore be a candidate substrate for both impulsivity-related temperaments and as a cortical biomarker for clinical disorders of impulse control.

Accumulating evidence indicates that the ventromedial PFC is critically involved in impulsive responding on the 5CSRTT and analogous measures of waiting impulsivity in both rodents and humans. Thus, physical lesions and pharmacological inactivation of this region enhance premature responding on both the 5CSRTT and analogous three-choice task in rats (Chudasama et al. 2003; Tsutsui-Kimura et al. 2014; Tsutsui-Kimura et al. 2016). Moreover, neural activity in this region encodes impulsive responses on both three-choice and two-choice variants of the 5CSRTT (Tsutsui-Kimura et al. 2016) while in humans impulsivity is related to cortical thickness (Merz et al. 2018) and activation (Christakou et al. 2011) of the ventromedial PFC. In neural connectivity terms, ventromedial PFC is posited to control impulsive urges through its rich connectivity with the NAc shell (Feja and Koch 2015) and by noradrenergic (Tsutsui-Kimura et al. 2014), cholinergic (Tsutsui-Kimura et al. 2010), glutamatergic (Benn and Robinson 2014) and GABAergic (Murphy et al. 2012) signaling. Our findings thus confirm the involvement of the IL cortex in anticipatory impulsive behavior and
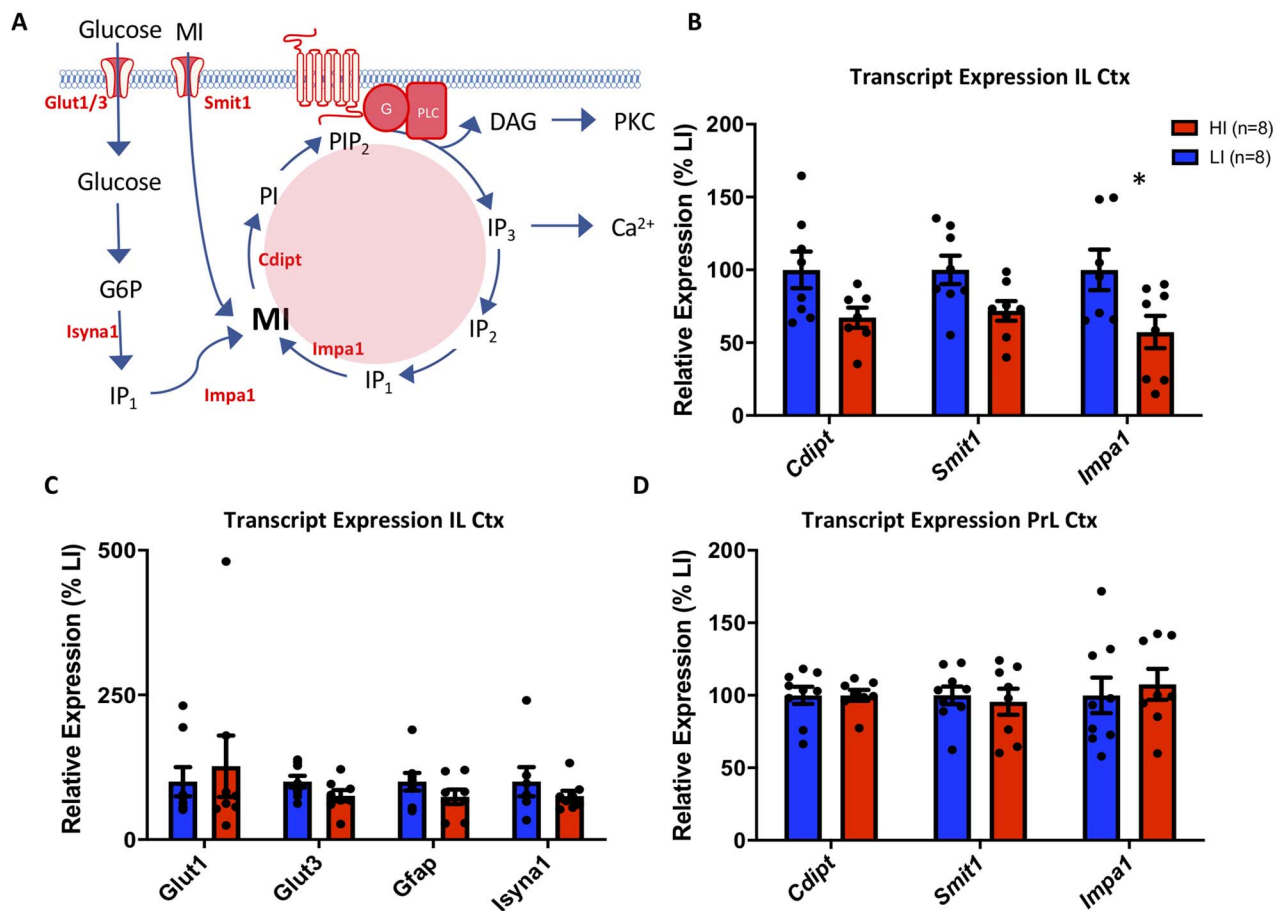
Figure 3. Transcript expression of genes related to the synthesis, uptake, and recycling of myoinositol and its precursor glucose, in high (HI) and low (LI) impulsive rats in the infralimbic and prelimbic cortex. (A) Inositol pathway showing de novo synthesis of myoinositol from its precursor, glucose, dietary uptake, and recycling through the IP3 pathway. Specific transcripts investigated are highlighted in red. (B) Transcript expression for enzymes involved in de novo synthesis (*Impa1*) and recycling (*Cdipt, Impa1*) through the IP_3 pathway and cellular uptake (*Smit1*) of dietary myoinositol were significantly reduced in the IL cortex of HI rats. Post hoc tests revealed a significant reduction in the expression of IMPase1 in the IL cortex of HI rats compared with LI ras (*$P < 0.01$). (C) No difference was observed in the expression of transcripts relating to the synthesis of myoinositol from glucose (*Isyna1*), glucose handling (*Glut1, Glut3*), or the glial marker *Gfap* between HI and LI rats in this region. (D) No difference was observed in the expression of transcripts relating to the synthesis and recycling of myoinositol through the IP3 pathway in the adjacent prelimbic cortex. Data are presented as a percentage of average transcript expression in LI rats. G6P—glucose-6-phosphate; MI—myoinositol; IP_3—Inositol-trisphosphate; IP_2—inositol-bisphosphate; IP_1—Inositol-monophosphate; PI—phosphotidylinositol; PIP_2—Phosphatidylinositol-bisphosphate, G—G protein, PLC—phospholipase C; DAG—diacylglycerol; PKC—protein kinase C.

highlight a putative mechanistic contribution of locally dysregulated myoinositol signaling in this region.

Myoinositol is an important component of membrane lipids with specific functions including osmoregulation (Fisher et al. 2002), autophagy (Sarkar and Rubinsztein 2006), and as a substrate in the IP_3 signal transduction pathway, the latter mediating an array of cellular processes important for neuronal functions relating to calcium signaling and homeostasis (reviewed in (Berridge 2009)). Although myoinositol is generally considered a glial marker (Brand et al. 1993), there is also evidence for its presence in neurons (Novak et al. 1999) where it is produced and regulated by several distinct processes (see Fig. 3A). These include the transport of dietary precursors across plasma membranes, a process controlled by SMIT; de novo synthesis from glucose-6-phosphate involving ISYNA and IMPase1, recycling via the IP_3 pathway mediated by CDIPT and IMPase1, and myoinositol efflux controlled by a volume-sensitive organic osmolyte channel (Rae 2014). Our findings suggest that high impulsivity may be caused in part by abnormalities in either de

novo synthesis of myoinositol and/or its recycling via the IP_3 pathway. Thus, the differentially reduced levels of myoinositol we observed in the IL cortex of HI rats were also accompanied by locally decreased transcript levels of IMPase1. These changes were regionally and neurochemically selective with no significant changes in transcript levels of proteins involved in the metabolism and turnover of myoinositol in the adjacent prelimbic cortex. Further, given that we observed no differences in GFAP transcript levels, n-acetyl-aspartate (an osmolyte and neuronal marker) or glucose content between HI and LI animals, the observed deficiency in myoinositol was unlikely to have been caused by deficits in glial function, neuronal density, glucose metabolism, or osmoregulation. It should be noted, however, that our capacity to detect the precise regional locus of reduced myoinositol concentration using ^{1}H-MRS was somewhat limited with the contrast between HI and LI rats failing to survive correction for multiple comparisons. This limitation most likely reflected the relatively large voxel size used compared with the more restricted IL subregion, limiting the sensitivity of our
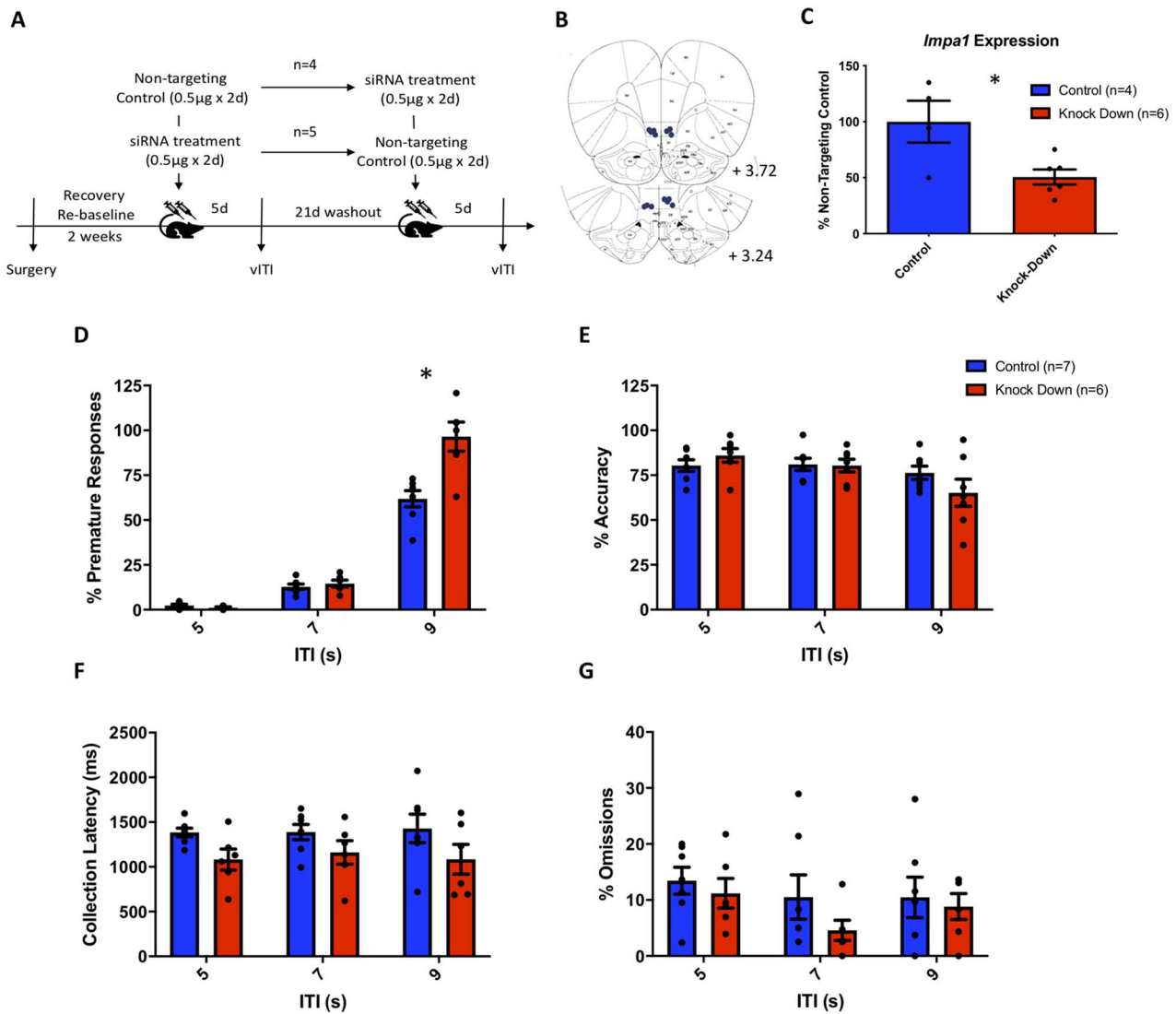
Figure 4. SiRNA-mediated knockdown of *Impa1* transcript expression in the IL cortex increased premature responding in the 5CSRTT. (*A*) Study design. Following surgical implantation of a guide cannula targeting the IL cortex, animals were retrained on the 5CSRTT prior to receiving bilateral infusions of siRNA targeting IMPase1 or a nontargeting control siRNA over two consecutive days and assessed 5 days later on a vITI schedule. After a washout period of 21 days, animals received the second intervention (siRNA targeting or nontargeting IMPase1) and were again assessed with a vITI challenge session. (*B*) Injector tip locations within the IL cortex of rats treated with siRNA. (*C*) Knockdown siRNA treatment significantly reduced *Impa1* expression in the IL cortex compared with nontargeting control siRNA. (*D*) A significant effect of siRNA knockdown was observed for premature responding during a variable vITI challenge, specifically when the ITI was increased to 9 sec, (*E–G*) No effect of siRNA treatment was observed on task accuracy, collection latency or omissions. * denotes $P < 0.05$, control $n = 5$, knockdown $n = 7$.

approach, which was further compounded by our relatively small sample size. Nevertheless, we were able to demonstrate the sufficiency of knockdown of IMPase1 transcript expression within the IL cortex to enhance impulsive responding on the 5CSRTT, suggesting that the observed reduction in myoinositol concentration was causally related to the expression of impulsivity in HI rats. Although it should be acknowledged that we did not directly measure myoinositol levels following local knockdown of IMPase1 activity this has previously been verified (Pettegrew et al. 2001).

The effect of IMPase1 knockdown on premature responding was found to be restricted to only the longest ITI trial, suggesting an effect of myoinositol deficiency on premature responding only under conditions of uncertainty, given the extended exposure of the rats to both the 5s SITI and 7s LITI conditions prior to

siRNA treatment. In keeping with this hypothesis, no difference in impulsive responding was observed for premature responding during the SITI screening sessions between HI and LI rats.

There has been renewed interest in understanding the mechanism of action of lithium in lowering impulsivity in mania, bipolar disorder, and other psychiatric disorders. In rodent tasks of impulsivity, lithium and the lithium-mimetic compound ebselen dose-dependently reduced impulsive behavior (Ohmura et al. 2012; Halcomb et al. 2013; Barkus et al. 2018), an action believed to be mediated by a reduction in cortical myoinositol levels (Lan et al. 2009), secondary to IMPase1 inhibition (Hallcher and Sherman 1980; Agam et al. 2009; Berridge 2009; Sade et al. 2016). However, given our present findings of diminished myoinositol levels in highly impulsive rats and the observed effect of IMPase 1 inhibition

in the IL cortex to increase impulsivity, it appears unlikely that lithium's effect to reduce impulsivity occurred as a result of diminished cortical myoinositol levels. Indeed, beyond its effects on IMPase1 activity, lithium also inhibits glycogen synthase kinase 3 (Jope 2003), an enzyme involved in many central intracellular pathways and linked with increased impulsivity in bipolar disorder (Jimenez et al. 2014). Alternatively, since both lithium and ebselen exert inhibitory effects on 5-HT2A receptor signaling (Goodwin et al. 1986; Antoniadou et al. 2018) and that 5-HT2A receptor antagonists decrease premature responding in the 5CSRTT (Passetti et al. 2003; Winstanley et al. 2004), lithium and related compounds may act via 5-HT receptor-dependent mechanisms to reduce impulsivity. Supporting this possibility, the mood stabilizer valproate decreases myoinositol synthesis (O'Donnell et al. 2003) and increases the expression of 5HT2A receptors (Sullivan et al. 2004) but has no effect on impulsive responding in the analogous 3CSRTT (Ohmura et al. 2012). Thus, it appears that lithium and related compounds decrease impulsivity by a mechanism independent of myoinositol signalling, potentially via effects on the 5HT2A receptor.

The present findings are compatible with ^{1}H-MRS studies reporting reduced levels of myoinositol in the PFC of various neuropsychiatric patient groups linked to impulsivity, including ADHD (Ferreira et al. 2009), depression (Coupland et al. 2005), schizophrenia (Shimon et al. 1998; Das et al. 2018), and substance use disorder (Durazzo et al. 2016; Murray et al. 2016). Importantly for this finding, therapeutics used to treat disorders of impulsivity such as methylphenidate (Quansah et al. 2017) and d-amphetamine (Barkai 1981) reportedly increase myoinositol levels in the human brain. Thus, our findings may have translational significance for understanding the pathophysiology of impulsivity-related disorders as well as the mechanism of action of clinically efficacious drugs. In defining this mechanism it is perhaps relevant to note that the IL cortex, corresponding to BA25 in humans, is widely implicated in negative affect (Myers-Schulz and Koenigs 2012), not only as an important neural locus linking emotionality with impulsive behavior (i.e., negative urgency) (e.g., Cyders et al. 2014; Hoptman et al. 2014) but also the integration of subjective reward-related information needed for appropriate decision-making (Mason et al. 2014). Thus, impaired myoinositol signaling in the IL cortex or its functional homologue in humans may predispose individuals to risky, impulsive decision-making under conditions of negative emotional state.

Conclusions

Using in-vivo ^{1}H-MRS, ex-vivo neurochemistry, and a complementary behavioral analysis, we report a novel role for myoinositol within the IL cortex in regulating impulsive behavior in rats. Based on our findings, this involvement may include deficits in the denovo synthesis of myoinositol and/or its recycling through the IP$_3$ pathway. This research confirms the importance of the IL cortex in regulating one form of "waiting impulsivity" and provides a putative mechanistic explanation and cortical biomarker of trait-like impulsivity, with clinical implications for such neuropsychiatric disorders as ADHD and substance use disorder.

Disclosures

Notes

References

Agam G, Bersudsky Y, Berry GT, Moechars D, Lavi-Avnon Y, Belmaker RH. 2009. Knockout mice in understanding the mechanism of action of lithium. *Biochem Soc Trans*. 37:1121–1125.

Antoniadou I, Kouskou M, Arsiwala T, Singh N, Vasudevan SR, Fowler T, Cadirci E, Churchill GC, Sharp T. 2018. Ebselen has lithium-like effects on central 5-HT2A receptor function. *Br J Pharmacol*. 175:2599–2610.

Bari A, Dalley JW, Robbins TW. 2008. The application of the 5-choice serial reaction time task for the assessment of visual attentional processes and impulse control in rats. *Nat Protoc*. 3:759–767.

Barkai AI. 1981. Myo-inositol turnover in the intact rat brain: increased production after d-amphetamine. *J Neurochem*. 36:1485–1491.

Barkus C, Ferland JN, Adams WK, Churchill GC, Cowen PJ, Bannerman DM, Rogers RD, Winstanley CA, Sharp T. 2018. The putative lithium-mimetic ebselen reduces impulsivity in rodent models. *J Psychopharmacol*. 32:1018–1026.

Batassa EM, Costanzi M, Saraulli D, Scardigli R, Barbato C, Cogoni C, Cestari V. 2010. RISC activity in hippocampus is essential for contextual memory. *Neurosci Lett*. 471:185–188.

Belin D, Mar AC, Dalley JW, Robbins TW, Everitt BJ. 2008. High impulsivity predicts the switch to compulsive cocaine-taking. *Science*. 320:1352–1355.

Belin-Rauscent A, Daniel ML, Puaud M, Jupp B, Sawiak S, Howett D, McKenzie C, Caprioli D, Besson M, Robbins TW et al. 2016. Impulsivity is predicted by the thinness of the insular cortex in rats. *Mol Psychiatry*. 21:445.

Benn A, Robinson ES. 2014. Investigating glutamatergic mechanism in attention and impulse control using rats in a modified 5-choice serial reaction time task. *PLoS One*. 9:e115374.

Berridge MJ. 2009. Inositol trisphosphate and calcium signalling mechanisms. *Biochim Biophys Acta*. 1793:933–940.

Boy F, Evans CJ, Edden RA, Lawrence AD, Singh KD, Husain M, Sumner P. 2011. Dorsolateral prefrontal gamma-aminobutyric acid in men predicts individual differences in rash impulsivity. *Biol Psychiatry*. 70:866–872.

Brand A, Richter-Landsberg C, Leibfritz D. 1993. Multinuclear NMR studies on the energy metabolism of glial and neuronal cells. *Dev Neurosci*. 15:289–298.

Caprioli D, Sawiak SJ, Merlo E, Theobald DE, Spoelder M, Jupp B, Voon V, Carpenter TA, Everitt BJ, Robbins TW et al.

2014. Gamma aminobutyric acidergic and neuronal structural markers in the nucleus accumbens core underlie trait-like impulsive behavior. *Biol Psychiatry*. 75:115–123.

Cardinal RN, Aitken MR. 2010. Whisker: a client-server high-performance multimedia research control system. *Behav Res Methods*. 42:1059–1071.

Christakou A, Brammer M, Rubia K. 2011. Maturation of limbic corticostriatal activation and connectivity associated with developmental changes in temporal discounting. *NeuroImage*. 54:1344–1354.

Chudasama Y, Passetti F, Rhodes SE, Lopian D, Desai A, Robbins TW. 2003. Dissociable aspects of performance on the 5-choice serial reaction time task following lesions of the dorsal anterior cingulate, infralimbic and orbitofrontal cortex in the rat: differential effects on selectivity, impulsivity and compulsivity. *Behav Brain Res*. 146:105–119.

Coupland NJ, Ogilvie CJ, Hegadoren KM, Seres P, Hanstock CC, Allen PS. 2005. Decreased prefrontal Myo-inositol in major depressive disorder. *Biol Psychiatry*. 57:1526–1534.

Cyders MA, Dzemidzic M, Eiler WJ, Coskunpinar A, Karyadi K, Kareken DA. 2014. Negative urgency and ventromedial prefrontal cortex responses to alcohol cues: FMRI evidence of emotion-based impulsivity. *Alcohol Clin Exp Res*. 38:409–417.

Dalley JW, Ersche KD. 2019. Neural circuitry and mechanisms of waiting impulsivity: relevance to addiction. *Philos Trans R Soc Lond Ser B Biol Sci*. 374:20180145.

Dalley JW, Everitt BJ, Robbins TW. 2011. Impulsivity, compulsivity, and top-down cognitive control. *Neuron*. 69:680–694.

Dalley JW, Fryer TD, Brichard L, Robinson ES, Theobald DE, Laane K, Pena Y, Murphy ER, Shah Y, Probst K *et al*. 2007. Nucleus accumbens D2/3 receptors predict trait impulsivity and cocaine reinforcement. *Science*. 315:1267–1270.

Dalley JW, Robbins TW. 2017. Fractionating impulsivity: neuropsychiatric implications. *Nat Rev Neurosci*. 18:158–171.

Dalley JW, Roiser JP. 2012. Dopamine, serotonin and impulsivity. *Neuroscience*. 215:42–58.

Dalley JW, Theobald DE, Pereira EA, Li PM, Robbins TW. 2002. Specific abnormalities in serotonin release in the prefrontal cortex of isolation-reared rats measured during behavioural performance of a task assessing visuospatial attention and impulsivity. *Psychopharmacology*. 164:329–340.

Das TK, Dey A, Sabesan P, Javadzadeh A, Theberge J, Radua J, Palaniyappan L. 2018. Putative astroglial dysfunction in schizophrenia: a meta-analysis of (1)H-MRS studies of medial prefrontal Myo-inositol. *Front Psych*. 9:438.

Diergaarde L, Pattij T, Poortvliet I, Hogenboom F, de Vries W, Schoffelmeer AN, De Vries TJ. 2008. Impulsive choice and impulsive action predict vulnerability to distinct stages of nicotine seeking in rats. *Biol Psychiatry*. 63:301–308.

Durazzo TC, Meyerhoff DJ, Mon A, Abe C, Gazdzinski S, Murray DE. 2016. Chronic cigarette smoking in healthy middle-aged individuals is associated with decreased regional brain N-acetylaspartate and glutamate levels. *Biol Psychiatry*. 79:481–488.

Economidou D, Pelloux Y, Robbins TW, Dalley JW, Everitt BJ. 2009. High impulsivity predicts relapse to cocaine-seeking after punishment-induced abstinence. *Biol Psychiatry*. 65: 851–856.

Ersche KD, Turton AJ, Pradhan S, Bullmore ET, Robbins TW. 2010. Drug addiction endophenotypes: impulsive versus sensation-seeking personality traits. *Biol Psychiatry*. 68:770–773.

Evenden JL. 1999. Varieties of impulsivity. *Psychopharmacology*. 146:348–361.

Feja M, Koch M. 2015. Frontostriatal systems comprising connections between ventral medial prefrontal cortex and nucleus accumbens subregions differentially regulate motor impulse control in rats. *Psychopharmacology*. 232:1291–1302.

Ferreira PE, Palmini A, Bau CH, Grevet EH, Hoefel JR, Rohde LA, Anes M, Ferreira EE, Belmonte-de-Abreu P. 2009. Differentiating attention-deficit/hyperactivity disorder inattentive and combined types: a (1)H-magnetic resonance spectroscopy study of fronto-striato-thalamic regions. *J Neural Transm (Vienna)*. 116:623–629.

Fisher SK, Novak JE, Agranoff BW. 2002. Inositol and higher inositol phosphates in neural tissues: homeostasis, metabolism and functional significance. *J Neurochem*. 82:736–754.

Gabbott PL, Warner TA, Jays PR, Salway P, Busby SJ. 2005. Prefrontal cortex in the rat: projections to subcortical autonomic, motor, and limbic centers. *J Comp Neurol*. 492:145–177.

Godlewska BR, Clare S, Cowen PJ, Emir UE. 2017. Ultra-high-field magnetic resonance spectroscopy in psychiatry. *Front Psych*. 8:123.

Goodwin GM, DeSouza RJ, Wood AJ, Green AR. 1986. Lithium decreases 5-HT1A and 5-HT2 receptor and alpha 2-adrenoceptor mediated function in mice. *Psychopharmacology*. 90:482–487.

Griffin JL, Bollard M, Nicholson JK, Bhakoo K. 2002. Spectral profiles of cultured neuronal and glial cells derived from HRMAS (1)H NMR spectroscopy. *NMR Biomed*. 15:375–384.

Halcomb ME, Gould TD, Grahame NJ. 2013. Lithium, but not valproate, reduces impulsive choice in the delay-discounting task in mice. *Neuropsychopharmacology*. 38:1937–1944.

Hallcher LM, Sherman WR. 1980. The effects of lithium ion and other agents on the activity of myo-inositol-1-phosphatase from bovine brain. *J Biol Chem*. 255:10896–10901.

Hoptman MJ, Antonius D, Mauro CJ, Parker EM, Javitt DC. 2014. Cortical thinning, functional connectivity, and mood-related impulsivity in schizophrenia: relationship to aggressive attitudes and behavior. *Am J Psychiatry*. 171:939–948.

Jentsch JD, Taylor JR. 1999. Impulsivity resulting from frontostriatal dysfunction in drug abuse: implications for the control of behavior by reward-related stimuli. *Psychopharmacology*. 146:373–390.

Jimenez E, Arias B, Mitjans M, Goikolea JM, Roda E, Ruiz V, Perez A, Saiz PA, Garcia-Portilla MP, Buron P *et al*. 2014. Association between GSK3beta gene and increased impulsivity in bipolar disorder. *Eur Neuropsychopharmacol*. 24:510–518.

Jope RS. 2003. Lithium and GSK-3: one inhibitor, two inhibitory actions, multiple outcomes. *Trends Pharmacol Sci*. 24:441–443.

Jupp B, Caprioli D, Saigal N, Reverte I, Shrestha S, Cumming P, Everitt BJ, Robbins TW, Dalley JW. 2013. Dopaminergic and GABA-ergic markers of impulsivity in rats: evidence for anatomical localisation in ventral striatum and prefrontal cortex. *Eur J Neurosci*. 37:1519–1528.

Karatas H, Erdener SE, Gursoy-Ozdemir Y, Lule S, Eren-Kocak E, Sen ZD, Dalkara T. 2013. Spreading depression triggers headache by activating neuronal Panx1 channels. *Science*. 339:1092–1095.

Lan MJ, McLoughlin GA, Griffin JL, Tsang TM, Huang JT, Yuan P, Manji H, Holmes E, Bahn S. 2009. Metabonomic analysis identifies molecular changes associated with the pathophysiology and drug treatment of bipolar disorder. *Mol Psychiatry*. 14:269–279.

Mason L, O'Sullivan N, Montaldi D, Bentall RP, El-Deredy W. 2014. Decision-making and trait impulsivity in bipolar disorder are associated with reduced prefrontal regulation of striatal reward valuation. *Brain*. 137:2346–2355.

Merz EC, He X, Noble KG, Pediatric Imaging N, Genetics S. 2018. Anxiety, depression, impulsivity, and brain structure in children and adolescents. *Neuroimage Clin*. 20:243–251.

Moeller FG, Barratt ES, Dougherty DM, Schmitz JM, Swann AC. 2001. Psychiatric aspects of impulsivity. *Am J Psychiatry*. 158:1783–1793.

Murphy ER, Fernando AB, Urcelay GP, Robinson ES, Mar AC, Theobald DE, Dalley JW, Robbins TW. 2012. Impulsive behaviour induced by both NMDA receptor antagonism and GABAA receptor activation in rat ventromedial prefrontal cortex. *Psychopharmacology*. 219:401–410.

Murray DE, Durazzo TC, Schmidt TP, Abe C, Guydish J, Meyerhoff DJ. 2016. Frontal metabolite concentration deficits in opiate dependence relate to substance use, cognition, and self-regulation. *J Addict Res Ther*. 7:pii: 286.

Myers-Schulz B, Koenigs M. 2012. Functional anatomy of ventromedial prefrontal cortex: implications for mood and anxiety disorders. *Mol Psychiatry*. 17:132–141.

Naaijen J, Lythgoe DJ, Amiri H, Buitelaar JK, Glennon JC. 2015. Fronto-striatal glutamatergic compounds in compulsive and impulsive syndromes: a review of magnetic resonance spectroscopy studies. *Neurosci Biobehav Rev*. 52:74–88.

Novak JE, Turner RS, Agranoff BW, Fisher SK. 1999. Differentiated human NT2-N neurons possess a high intracellular content of myo-inositol. *J Neurochem*. 72:1431–1440.

O'Donnell T, Rotzinger S, Nakashima TT, Hanstock CC, Ulrich M, Silverstone PH. 2003. Chronic lithium and sodium valproate both decrease the concentration of myoinositol and increase the concentration of inositol monophosphates in rat brain. *Eur Neuropsychopharmacol*. 13:199–207.

Ohmura Y, Tsutsui-Kimura I, Kumamoto H, Minami M, Izumi T, Yamaguchi T, Yoshida T, Yoshioka M. 2012. Lithium, but not valproic acid or carbamazepine, suppresses impulsive-like action in rats. *Psychopharmacology*. 219:421–432.

Passetti F, Dalley JW, Robbins TW. 2003. Double dissociation of serotonergic and dopaminergic mechanisms on attentional performance using a rodent five-choice reaction time task. *Psychopharmacology*. 165:136–145.

Pattij T, Vanderschuren LJ. 2008. The neuropharmacology of impulsive behaviour. *Trends Pharmacol Sci*. 29:b192–199.

Paxinos G, Watson C. 2007. In: Paxinos G, Watson C, editors. *The rat brain in stereotaxic coordinates*. Amsterdam: Elsevier.

Pettegrew JW, Panchalingam K, McClure RJ, Gershon S, Muenz LR, Levine J. 2001. Effects of chronic lithium administration on rat brain phosphatidylinositol cycle constituents, membrane phospholipids and amino acids. *Bipolar Disord*. 3: 189–201.

Provencher SW. 2001. Automatic quantitation of localized in vivo 1H spectra with LCModel. *NMR Biomed*. 14:260–264.

Quansah E, Ruiz-Rodado V, Grootveld M, Probert F, Zetterstrom TSC. 2017. (1)H NMR-based metabolomics reveals neurochemical alterations in the brain of adolescent rats following acute methylphenidate administration. *Neurochem Int*. 108:109–120.

Rae CD. 2014. A guide to the metabolic pathways and function of metabolites observed in human brain 1H magnetic resonance spectra. *Neurochem Res*. 39:1–36.

Robinson ES, Eagle DM, Economidou D, Theobald DE, Mar AC, Murphy ER, Robbins TW, Dalley JW. 2009. Behavioural characterisation of high impulsivity on the 5-choice serial reaction time task: specific deficits in 'waiting' versus 'stopping. *Behav Brain Res*. 196:310–316.

Sade Y, Toker L, Kara NZ, Einat H, Rapoport S, Moechars D, Berry GT, Bersudsky Y, Agam G. 2016. IP3 accumulation and/or inositol depletion: two downstream lithium's effects that may mediate its behavioral and cellular changes. *Transl Psychiatry*. 6:e968.

Sarkar S, Rubinsztein DC. 2006. Inositol and IP3 levels regulate autophagy: biology and therapeutic speculations. *Autophagy*. 2:132–134.

Schachar R, Logan GD, Robaey P, Chen S, Ickowicz A, Barr C. 2007. Restraint and cancellation: multiple inhibition deficits in attention deficit hyperactivity disorder. *J Abnorm Child Psychol*. 35:229–238.

Shimon H, Sobolev Y, Davidson M, Haroutunian V, Belmaker RH, Agam G. 1998. Inositol levels are decreased in post-mortem brain of schizophrenic patients. *Biol Psychiatry*. 44: 428–432.

Sullivan NR, Burke T, Siafaka-Kapadai A, Javors M, Hensler JG. 2004. Effect of valproic acid on serotonin-2A receptor signaling in C6 glioma cells. *J Neurochem*. 90:1269–1275.

Tsutsui-Kimura I, Ohmura Y, Izumi T, Matsushima T, Amita H, Yamaguchi T, Yoshida T, Yoshioka M. 2016. Neuronal codes for the inhibitory control of impulsive actions in the rat infralimbic cortex. *Behav Brain Res*. 296:361–372.

Tsutsui-Kimura I, Ohmura Y, Izumi T, Yamaguchi T, Yoshida T, Yoshioka M. 2010. Nicotine provokes impulsive-like action by stimulating alpha4beta2 nicotinic acetylcholine receptors in the infralimbic, but not in the prelimbic cortex. *Psychopharmacology*. 209:351–359.

Tsutsui-Kimura I, Yoshida T, Ohmura Y, Izumi T, Yoshioka M. 2014. Milnacipran remediates impulsive deficits in rats with lesions of the ventromedial prefrontal cortex. *Int J Neuropsychopharmacol*. 18.

Uylings HB, Groenewegen HJ, Kolb B. 2003. Do rats have a prefrontal cortex? *Behav Brain Res*. 146:3–17.

Vertes RP. 2004. Differential projections of the infralimbic and prelimbic cortex in the rat. *Synapse*. 51:32–58.

Voon V, Dalley JW. 2016. Translatable and back-translatable measurement of impulsivity and compulsivity: convergent and divergent processes. *Curr Top Behav Neurosci*. 28:53–91.

Winstanley CA, Eagle DM, Robbins TW. 2006. Behavioral models of impulsivity in relation to ADHD: translation between clinical and preclinical studies. *Clin Psychol Rev*. 26:379–395.

Winstanley CA, Theobald DE, Dalley JW, Glennon JC, Robbins TW. 2004. 5-HT2A and 5-HT2C receptor antagonists have opposing effects on a measure of impulsivity: interactions with global 5-HT depletion. *Psychopharmacology*. 176:376–385.

Yoo CH, Lim SI, Song KH, Woo DC, Choe BY. 2018. Investigating the metabolic alterations in a depressive-like rat model of chronic forced swim stress: an in vivo proton magnetic resonance spectroscopy study at 7T. *Neurochem Int*. 116:22–29.